Diffraction of Neutral Helium Clusters: Evidence for "Magic Numbers"

Rüdiger Brühl,[1,*] Rafael Guardiola,[2] Anton Kalinin,[1] Oleg Kornilov,[1] Jesús Navarro,[3] Tim Savas,[4] and J. Peter Toennies[1]

[1]*Max-Planck-Institut für Strömungsforschung, Bunsenstraße 10, 37073 Göttingen, Germany*
[2]*Departamento de Física Atómica y Nuclear, Facultad de Física, 46100 Burjassot, Spain*
[3]*IFIC (CSIC-Universidad de Valencia), Apartado 22085, 46071 Valencia, Spain*
[4]*Massachusetts Institute of Technology, Cambridge, Massachusetts 02139, USA*

(Received 19 December 2003; published 6 May 2004)

The size distributions of neutral ^{4}He clusters in cryogenic jet beams, analyzed by diffraction from a 100 nm period transmission grating, reveal magic numbers at $N = 10$–11, 14, 22, 26–27, and 44 atoms. Whereas magic numbers in nuclei and clusters are attributed to enhanced stabilities, this is not expected for quantum fluid He clusters on the basis of numerous calculations. These magic numbers occur at threshold sizes for which the quantized excitations calculated with the diffusion Monte Carlo method are stabilized, thereby providing the first experimental confirmation for the energy levels of ^{4}He clusters.

DOI: 10.1103/PhysRevLett.92.185301 PACS numbers: 67.40.Db, 36.40.–c

In cluster physics, as in nuclear physics, magic numbers corresponding to anomalies in the abundance of particles with a particular size N have attracted considerable attention. Invariably they provide direct evidence for quantized finite size effects. For neutral clusters the magic numbers found previously can, generally speaking, be related to enhanced ground state stabilities at the completion of structural shells, as in van der Waals clusters. From the spacing of the observed magic numbers important conclusions about the solid state structures can be obtained [1]. In the case of metal clusters magic numbers appear whenever the valence electrons fill the corresponding closed shells [2]. As opposed to all other clusters studied so far helium clusters are the only ones which are definitely liquidlike. Since liquid helium is the only known bulk superfluid, helium clusters have long been studied theoretically as a model for investigating size effects in a many-body quantum fluid. Both simulations [3] and experiment [4] have established the superfluidity for ^{4}He clusters with $N \gtrsim 60$. In addition many other ^{4}He cluster properties have been studied using a wide range of microscopic computational techniques [5]. Early speculations concerning magic numbers [6] were ruled out by these calculations which all predict a smooth behavior of the ground state properties with number size. One paper is even titled "No Magic Numbers in Neutral ^{4}He Clusters" [7].

In the present experiments diffraction from a nanostructured transmission grating is used to analyze the number size distribution of helium clusters in a beam produced by a cryogenic free jet expansion [8]. Via the de Broglie wavelength the diffraction angle depends inversely on the cluster mass. This method has the big advantage over techniques such as electron-impact mass spectrometry that it is essentially nondestructive. Previously it was found that cluster distributions in the beam were dominated by intense dimer and trimer peaks [9]. This was unexpected in view of their extraordinary weak binding [10] but is now understood in terms of strongly quantum enhanced three-body recombination cross sections [9]. In the new experiments reported here individual clusters differing by one atom can now be resolved up to about $N = 21$ [11]. Moreover, the resulting cluster size distributions exhibit maxima corresponding to most probable sizes of about 10–11, 14, 22, 26–27, and 44 not seen previously. The maxima are explained by the stabilization of an additional quantized elementary excitation state at certain sizes, which affects the partition functions and thus the equilibrium cluster populations in the formative stages of the expansion. These magic numbers provide the first direct information on the elementary excitations of small helium clusters in good agreement with diffusion Monte Carlo (DMC) calculations.

The new apparatus has a greater structural stability than the one described earlier [12], making it possible to replace the 10 μm slits used earlier by 5 μm slits, separated by 83 cm, and also to increase the distance from the grating to the 25 μm wide detector entrance slit from 45 to 130 cm (see the inset in Fig. 1). As a result the angular resolution is improved from about 70 μrad (FWHM) in the previous experiments to 20 μrad. The angular positioning of the detector has been improved to guarantee a repeatability within 1–2 μrad.

Figure 1(a) provides an overview of the new results for a source temperature of $T_0 = 6.7$ K ($\lambda_1 = 4.0$ Å) and a source pressure of $P_0 = 1.25$ bars, measured with the mass spectrometer set to detect He^+(4 amu) ion fragments produced by electron impact. At negative deflection angles the spectra encompass the region between the specular peak at $\theta = 0$ and the first order monomer peak at $\theta = -4.0$ mrad [13] where the first order diffraction peaks of the clusters are expected. According to

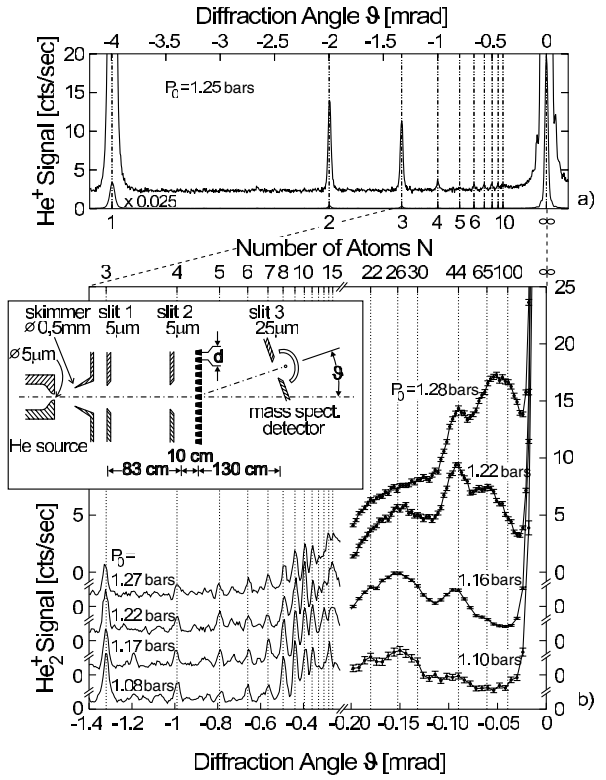

FIG. 1. Experimental helium cluster diffraction patterns measured at $T_0 = 6.7$ K (a) with the mass spectrometer set at mass 4 amu (He^+) and (b) with the mass spectrometer set at mass 8 amu (He_2^+) for different source pressures P_0. The intensity scale is the same for all the patterns in (b) except for a vertical shift of 3 counts/s. The effective overall angular resolution (FWHM) is 20 μrad as determined from the width of the specular peak. The numbers of atoms in the corresponding diffraction peaks are indicated in the bottom abscissa in (a) and in the top abscissa in (b). The inset shows the important dimensions of the apparatus.

Bragg's law the first order diffraction peaks are given by $\theta_N \approx \lambda_N/d = h(Nm_{\mathrm{He}}vd)^{-1}$, where N is the number size of the cluster, λ_N is its de Broglie wavelength, v is its velocity, and d is the period of the grating which in our case is 100 nm. Thus the dimer and the trimer, which dominate the diffraction pattern, appear, respectively, at $1/2$ and $1/3$ of the monomer diffraction angle. At small angles the sequence of additional resolved barely visible peaks corresponds to clusters with $N < 10$. At even smaller angles ($|\theta| \leq 0.1$ mrad) the diffraction pattern is obscured by secondary peaks resulting from the diffraction of the He atoms from the 5 μm collimating slit (see Ref. [45] in Ref. [9]). To avoid this undesired background the mass spectrometer is set to the mass of the He_2^+(8 amu) ion fragment, which is the dominant ion fragment of clusters with $N > 3$ [14]. The cluster signals are now greater by more than an order of magnitude (3–6 counts/s) and the background is only about 1 count/s so that individual clusters with $N \leq 11$ are clearly resolved [Fig. 1(b)]. The $N = 4$, 5, 6, and 7 signals are smaller compared to $N = 3$. At larger N, however, the peak intensities rise again and at $N = 9$–11 are clearly enhanced, followed by another maximum at about 14 and 15. Additional distinct maxima are seen at $N = 22$, 26, and 44 and also at about 65 for $P_0 = 1.22$ bars, and 75 for $P_0 = 1.28$ bars.

The magic number structures were unchanged on varying the electron-impact energies between 70 and 400 eV, inclining the grating by $\Theta_0 = 9.6^{\circ}$–19.2° with respect to the incident beam, and on modifying the source conditions to $T_0 = 4.1$ K and $P_0 = 0.385$ bar. These and other tests confirm that the observed structures are indeed an intrinsic property of the gas expansions and do not depend on the way the beam is detected in the experiment.

In order to interpret the features in terms of cluster sizes it is necessary to know their velocities. The sharpness and positions of the resolved diffraction peaks for $N \leq 11$ confirm that these clusters all have the same velocities v and the same FWHM of $\Delta v/v < 1\%$. Time-of-flight distributions of the undiffracted beam containing larger clusters, measured on mass 8 amu over a wide range of pressures, also revealed only a slight decrease in velocities by only about 3% due to real gas effects [9] and a velocity FWHM less than 1%. Thus the diffraction angles at $|\theta| \leq 0.5$ mrad are assigned with confidence to the corresponding cluster sizes even though they are not individually resolved.

More insight into the actual magnitudes of the magic number maxima is provided by transforming the angular distributions to the true population distributions in the beam. This requires the following corrections: (i) The probability that the corresponding He_2^+ fragment ion is formed upon ionization of a given neutral cluster must be known. This was measured previously to be 5%, 40%, 70%, 70%, and 75% for $N = 2$–6, respectively [9]. For larger clusters with $N \approx 100$ there is evidence that 70% of the cluster ion fragments are He_2^+ [15]. Thus the He_2^+ distribution measured on mass 8, I_8, provides a signal proportional to the intensity of the neutral clusters for all N. (ii) The ionization cross sections were estimated to be proportional to N in agreement with Ref. [16]. (iii) The relative diffraction intensities are also affected by the reduction of the effective slit width due to the van der Waals interactions with the grating walls. This effect was estimated from the theory in Ref. [10]. After these corrections the population distributions $G(N)$ for $N > 11$ were calculated from the modified angular distributions $I_8^*(\theta)$ via the simple formula

$$G(N(\theta)) = I_8^*(\theta)\left|\frac{d\theta}{dN}\right| \propto I_8^*(\theta)N^{-2}, \qquad (1)$$

since from Bragg's law the Jacobian is $|d\theta/dN| \propto N^{-2}$. In the resolved part of the spectrum ($N \leq 11$) the areas under the peaks were used.

Figure 2 compares the $G(N)$ distributions derived from the experimental diffraction patterns presented in Fig. 1(b) with best fit log-normal distributions. The good average agreement with the log-normal distributions is gratifying since it has been predicted by theoretical models of cluster growth [17] and has previously been observed only in less direct deflection scattering measurements of helium droplets with $N > 1000$ [18]. Figure 2(b) shows the ratios of the actual $G(N)$ distributions to the smooth log-normal distributions. These ratios provide a true measure of the magic number effect on the cluster size distributions and clearly reveal the magic numbers listed in Table I. It is important to note that the broad maxima at $N = 65$ ($P_0 = 1.22$ bars) and $N = 75$ ($P_0 = 1.28$ bars) in Fig. 1(b) are not magic numbers but artifacts found only at the highest source pressures. These maxima can be explained by noting that the angular distributions corresponding to smooth $G(N)$ distributions have to be multiplied by a factor of N^3.

The magic numbers are explained by analyzing the growth of clusters in the early "hot" stages of the expansion under near-equilibrium conditions. Model calculations have established that anomalies in the equilibrium constants of reactions involving a particular cluster size can produce magic numbers in the otherwise smooth distribution of cluster sizes [19]. For an assumed growth reaction $He_{N-1} + He + He \rightarrow He_N + He$ the equilibrium constant is given by

$$K_N = \frac{Z_N}{Z_{N-1} Z_1}, \tag{2}$$

where the partition functions Z_N are expressed as products of center-of-mass (z_N) and internal (ξ_N) partition functions by $Z_N = z_N \xi_N$ with $z_N = N^{3/2} Z_1$. The internal partition functions are given in terms of the $j_N + 1$ bound state energy levels E_j of the N-atom cluster by

$$\xi_N = \sum_{j=0}^{j_N} g_j(N) \exp\left[-\frac{E_j(N)}{kT} \right], \tag{3}$$

where the degeneracy factor for the state $j = (n, \ell)$ with the radial quantum number n and angular momentum ℓ is given by $g_j = 2\ell + 1$.

To implement Eqs. (2) and (3) it is necessary to know both the chemical potential, which is the binding energy of one atom to the cluster, and the energies of excited levels characterized by (n, ℓ), where n describes the radial excitation and ℓ is the angular momentum of the cluster. These energies were systematically computed by the DMC method for each N between 3 and 50. The angular momentum ℓ is imposed on the importance sampling wave function by means of a factor $\sum_{i=1}^{N} f_\ell(r_i) \times P_\ell(\cos\theta_i)$, where P_ℓ is a Legendre polynomial, and the single-particle coordinates are referred to the center of mass to ensure translational invariance. The choice $f_\ell(r) = r^\ell$ was made for all ℓ, except $f_1(r) = r^3$. The DMC method provides the lowest energy for each of these ℓ subspaces, but due to the presence of nodal surfaces for $\ell > 0$, only upper bounds are actually obtained within the so-called fixed-node approximation. An optimized moment method [20] was used to show that only the (1, 0) (monopolar) excited state is bound and other additional excitations do not exist.

The calculated excitation energies agree with earlier calculations [21,22] for $\ell = 0, 2$ within statistical errors. All the energy levels and the chemical potential vary monotonically with the number N. For $N \leq 50$ the calculations indicate that neither the (0, 1) nor the $(1, \ell > 0)$ levels are bound and that the number of bound states

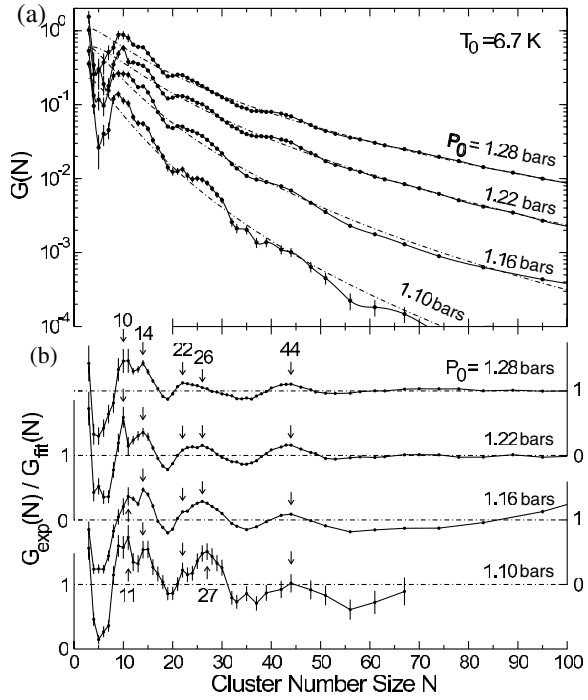

FIG. 2. (a) ^{4}He cluster size distributions $G(N)$ obtained from a transformation of the diffraction patterns in Fig. 1 as described in the text. The sharp drop-off in the average distributions at large sizes N is caused by the N^{-2} factor in the Jacobian of the transformation and the N^{-1} correction of the ionization cross section. (b) The ratio of the $G(N)$ distributions to the log-normal distributions [dot-dashed curves in (a)]. Maxima in the cluster size distributions are clearly seen at $N =$ 10–11, 14, 22, 26–27, and 44. The statistical errors are indicated by the vertical lines.

TABLE I. Comparison of experimental magic numbers determined from the angular distributions $I(\theta)$ and from the $G(N)$ distributions with the theoretical values Z_N/Z_{N-1}.

$I(\theta)$	9–10	14–15	22	25–27	42–46
$G(N)$	10–11	14	22	26–27	44
Z_N/Z_{N-1}	8 ± 1	14 ± 1	$\cdots$	25 ± 1	41 ± 1

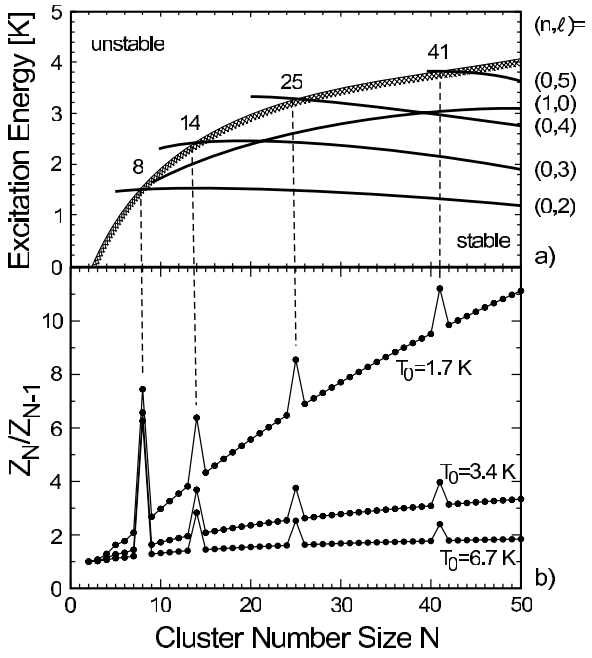

FIG. 3. (a) The energies E_j of the collective excitations for different values of the angular momentum and the chemical potential are plotted as a function of N. (b) The ratio of the partition functions Z_N/Z_{N-1} is plotted versus N. At the threshold values in (a) the ratio shows maxima.

$(n, \ell) = (0, 2), (0, 3) \ldots$ and $(1, 0)$ with energies below the chemical potential increases with N. To wash out the unavoidable statistical fluctuations, the calculated energies have been fitted to obtain the smooth curves displayed in Fig. 3(a). The partition functions calculated from these excitation energies increase smoothly with the number of particles, with the exception of the cases in which a new level is bound giving rise to a sudden step. When computing Z_N/Z_{N-1} this step is converted into a sharp maximum. The position of these maxima, Fig. 3(b), are in nice agreement with the experimental magic numbers (Table I), with the exception of the enhancement at $N = 22$ for which we have no explanation.

In conclusion, the nondestructive matter wave diffraction patterns with an improved mass resolution provide the first observation of "magic numbers" in ^{4}He clusters. These magic numbers are not related to enhanced ground state binding energies at specific values of N. They are, in fact, stability thresholds, related to the cluster sizes at which excited levels cross the chemical potential curve and become stabilized. As far as we are aware this is also the first experimental evidence for such a mechanism for the production of magic numbers. The results also confirm the predicted log-normal-like size distributions of cluster sizes formed in free jet expansions.

We thank E. Krotscheck for inspiring discussions and R. Düren and H. Walther for their support which made these experiments possible. R. G. and J. N. are supported by MCyT/FEDER (Spain), BMF2001-0262.

*Present address: Physikalisch-Technische Bundesanstalt, Abbestrasse 2-12, 10587 Berlin, Germany.

[1] See the reviews in *Clusters of Atoms and Molecules*, edited by H. Haberland (Springer, Berlin, 1994).
[2] W. A. de Heer, Rev. Mod. Phys. **65**, 611 (1993).
[3] P. Sindzingre, M. L. Klein, and D. M. Ceperley, Phys. Rev. Lett. **63**, 1601 (1989).
[4] S. Grebenev, J. P. Toennies, and A. F. Vilesov, Science **279**, 2083 (1998).
[5] See, for example, the reviews in *Microscopic Approaches to Quantum Liquids in Confined Geometries*, edited by E. Krotscheck and J. Navarro (World Scientific, Singapore, 2002).
[6] T. Regge, J. Low Temp. Phys. **9**, 123 (1972).
[7] R. Melzer and J. G. Zabolitzky, J. Phys. A **17**, L565 (1984).
[8] W. Schöllkopf and J. P. Toennies, Science **266**, 1345 (1994).
[9] L. Bruch, W. Schöllkopf, and J. P. Toennies, J. Chem. Phys. **117**, 1544 (2002).
[10] R. E. Grisenti, W. Schöllkopf, J. P. Toennies, G. C. Hegerfeldt, and T. Köhler, Phys. Rev. Lett. **83**, 1755 (1999).
[11] The ultimate resolution was achieved by tilting the grating with respect to the beam axis. This way the grating period is effectively reduced, which leads to an effective increase in resolution.
[12] R. E. Grisenti, W. Schöllkopf, J. P. Toennies, J. R. Manson, T. A. Savas, and H. I. Smith, Phys. Rev. A **61**, 033608 (2000).
[13] The data at positive angles are omitted since diffraction patterns are invariably symmetric with respect to the specular peak.
[14] W. Schöllkopf and J. P. Toennies, J. Chem. Phys. **104**, 1155 (1996).
[15] B. E. Callicoatt *et al.*, J. Chem. Phys. **109**, 10 195 (1998).
[16] F. Bottiglioni, J. Contant, and M. Fois, Phys. Rev. A **6**, 1830 (1972).
[17] M. Villarica, M. J. Casey, J. Goodisman, and J. Chaiken, J. Chem. Phys. **98**, 4610 (1993).
[18] M. Lewerenz, B. Schilling, and J. P. Toennies, Chem. Phys. Lett.. **206**, 381 (1993).
[19] J. Chaiken and J. Goodisman, J. Cluster Sci. **6**, 319 (1995).
[20] R. Guardiola, J. Navarro, and M. Portesi, Phys. Rev. B **63**, 224519 (2001).
[21] E. Krotscheck and S. Chin, Phys. Rev. B **52**, 10 405 (1995).
[22] D. Blume and C. H. Greene, J. Chem. Phys. **112**, 8053 (2000).